RADIATIVE TRANSFER IN SPHERICAL SHELL ATMOSPHERES

II. ASYMMETRIC PHASE FUNCTIONS

by

George W. Kattawar

Department of Physics

and

Charles N. Adams

Department of Electrical Engineering

and Department of Physics

Texas A&M University

College Station, Texas 77843

Report No. 37

The research described in this report was

funded by the

National Aeronautics and Space Administration

Grant No. NGR 44-001-117

September 22, 1977

A paper based on the material in this report has been submitted to Icarus.

RADIATIVE TRANSFER IN SPHERICAL SHELL ATMOSPHERES

II. ASYMMETRIC PHASE FUNCTIONS

by

George W. Kattawar
Department of Physics

and

Charles N. Adams
Department of Electrical Engineering
and Department of Physics
Texas A&M University

Abstract

In this paper we investigated the effects of sphericity on the radiation reflected from a planet with a homogeneous, conservative scattering atmosphere of optical thicknesses of 0.25 and 1.0. We considered a Henyey-Greenstein phase function with asymmetry factors of 0.5 and 0.7. Significant differences were found when these results were compared with the plane-parallel calculations. Also large violations of the reciprocity theorem, which is only true for plane-parallel calculations, were noted. Results are presented for the radiance versus height distributions as a function of planetary phase angle. These results will be useful to researchers in the field of remote sensing and planetary spectroscopy.

Introduction

In a recent paper by Adams and Kattawar (1977), hereafter referred to as part I, detailed comparisons were made between the plane-parallel approximation (PP) and the more realistic spherical shell atmosphere (SSA) calculation for a homogeneous, conservative, Rayleigh scattering atmosphere. In this paper large deviations between the PP and SSA cases were noted for certain angles of incidence and emergence. Also gross violations of reciprocity were found for certain angles using the SSA. It is the purpose of this paper to make similar comparisons for an atmosphere which has varying degrees of asymmetry in its phase function. To this end we have chosen to use the Henyey-Greenstein phase function (HG), namely

$$P(\xi) = \frac{1 - g^2}{4\pi(1 - 2g\xi + g^2)^{3/2}} \tag{1}$$

where ξ is the cosine of the scattering angle ($\cos \Theta$) and g is the asymmetry factor given by

$$\langle \xi \rangle = g = \int_{-1}^{1} \int_{0}^{2\pi} \xi P(\xi)\, d\phi\, d\xi \tag{2}$$

It should be noted that $P(\xi)$ is normalized to unity when integrated over 4π steradians.

Sampling the Phase Function

Let $\phi(\psi)$ be a uniform density function defined by

$$\phi(\psi) = \begin{cases} 1 & 0 \leq \psi \leq 1 \\ 0 & \text{otherwise} \end{cases} \tag{3}$$

also let $Q(\psi)$ be the distribution function of ξ defined by

$$Q(\psi) = \int_{-1}^{\psi} P'(\xi)d\xi \tag{4}$$

where

$$P'(\xi) = \frac{1 - g^2}{2(1 - 2g\xi + g^2)^{3/2}} \tag{5}$$

and

$$\int_{-1}^{1} P'(\xi)d\xi = 1 \tag{6}$$

Now it is clear that there exists an R and ψ such that

$$\int_{0}^{R} \phi(y)dy = Q(\psi) = R \tag{7}$$

since both density functions are normalized to unity. Now obtaining $Q(\psi)$ from eqs. (4) and (5) and solving for ψ in terms of R we get

$$\psi = \frac{1 + g^2 - [(g(2R - 1) + 1)/(1 - g^2)]^{-2}}{2g} \tag{8}$$

It should be noted that $\psi = -1$ when $R = 0$ and $\psi = 1$ when $R = 1$ and R is a random

number between zero and unity. In Fig. 1 we show how well the distribution of the variable ψ, obtained by sampling using eqn. (8), agrees with the theoretical density function for the cases where g = 0.5 and 0.7.

Calculational Results

For these calculations we have maintained the same model as was used in part I. In this study we only vary the asymmetry parameter g and we will consider two values, namely g = 0.5 and 0.7. It should be noted that in the case of Rayleigh scattering which was used in part I that $\langle\xi\rangle = 0$ but this does not correspond to the case of g = 0 for the HG phase function which is isotropic scattering. In Figs. 2a-2d we present results for the reflected radiance versus nadir angle for the cases where $\theta_0 = 0^0$; $\tau = 0.25$ and 1.0; g = 0.5 and 0.7. All nomenclature is the same as that used in part I of this series. The first thing to be noted is that the radiance for the SSA case is always greater than or equal to the PP case for all nadir angles less than the one for which I_{TS}^{SSA} reaches a maximum. This result is independent of the g parameter and is also true for Rayleigh scattering. To aid in interpreting the results for this and other figures we have constructed Tables 1 and 2 giving I_{SS}^{PP}, I_{SS}^{SSA}, $I_{SS}^{SSA}/I_{TS}^{SSA}$, and I_{SS}^{PP}/I_{TS}^{PP} for g = 0.5 and 0.7 respectively. If these tables are compared with the corresponding table in part I we note that multiple scattering is much more dominant for the cases where g = 0.5 and 0.7 than it is for Rayleigh scattering. The exceptions being at extreme nadir angles for $\tau = 0.25$. We also note that the greater the asymmetry factor the greater the effect of multiple scattering particularly for nadir angles greater than 70^0. Differences between the PP and SSA of 20% are still prevelant at $\tau = 0.25$ in the region where the SSA radiance peaks and diminish considerably as the optical depth increases to 1.0. The

matrix operator (MO) calculations are presented so that one could gain some insight into the statistical fluctuations in the results by comparing with the backward plane-parallel calculation (PP). In figs. 3a-d the solar incident angle is 70.47^{o}. To better understand the behavior depicted in this figure one should refer to Tables 1 and 2. Comparing similar cases for g = 0.5 and 0.7 we again see that slightly more multiple scattering exists for g = 0.7 than for g = 0.5. This difference is much more pronounced when g = 0.7 is compared to the similar case for Rayleigh scattering in part I, Table 1. Also note that for $\tau = 0.25$ and for angles greater than 80^{o} there is relatively more SS for the SSA than for the PP case while at all other angles they are comparable. Closer analysis of the data yields a very important result. We see that only when differences appear in the SS do we get differences in TS. It thus appears that differences in SS are a necessary condition for differences in TS. In Figs. 4a, 4b, 5a, 5b the solar zenith angle is increased further to 84.20^{o} for g = 0.5 and 0.7 respectively. If we again refer to Tables 1 and 2 we first note the fact that $I_{SS}^{PP} < I_{SS}^{SSA}$ for all nadir angles up to 85^{o}. This accounts for the fact that $I_{TS}^{PP} < I_{TS}^{SSA}$ for these angles since the ratio of SS/TS is comparable between the PP and SSA. There is also an extremely important result worth noting in this data and that is the fact I_{SS}^{SSA} for $\tau = 0.25$ can be greater than I_{SS}^{SSA} for $\tau = 1.0$. This result can not occur for the PP case since I_{SS}^{PP} is a monotonically increasing function of τ for fixed directions of incidence and emergence. This phenomenon is strictly due to curvature effects and more will be said about this when we present the radiance versus height distribution. Finally we observe again that as g increases the ratio of SS/TS decreases.

In Figs. 6a-d we present the radiance versus height distribution for both SS and MS for a pair of reciprocal points (θ, θ_0; 0, 60^0) and $\phi = 0^0$ for $\tau = 0.25$, 1.0 and g = 0.5, 0.7. These curves should be compared with Figs. 9 and 11 of part I for Rayleigh scattering. There are several noteworthy differences. First we observe that for Rayleigh scattering and $\tau = 0.25$ the SS contribution is <u>always</u> greater than the MS contribution. This is no longer true when we go to more asymmetric phase functions. In fact from 0-50 km the MS is comparable to the SS for g = 0.5 and 0.7. For the $\tau = 1.0$ case the MS dominates everywhere over SS for g = 0.5 and 0.7 whereas for Rayleigh scattering the MS exceeds the SS up to 88 km. Also the MS distribution is much broader for g = 0.5 and 0.7 than it is for Rayleigh scattering. This is due to fact that the forward peak in the phase function tends to inject the photons deeper into the atmosphere. Therefore if one looks at these results from a spectroscopist point of view then it becomes apparent that significantly different regions will be probed in an inhomogeneous atmosphere depending on the type of scattering taking place. In Fig. 7a we present the SS and MS versus height distribution for the cases where $\tau = 0.25$ and g = 0.5 for the following equal incident and emergent angles, $\theta = \theta_0 = 0^0$, 60^0, 83^0 and $\phi = 0^0$. These angles were chosen so that if one were viewing a planet from a spacecraft at a large distance then these angles would correspond to a point at the intensity equator on the mirror meridian at phase angles of 0^0, 120^0, and 166^0 respectively. We first see that as the phase angle increases the ratio of SS/TS increases; in fact these ratios are 55, 65, and 83% respectively. A most interesting feature in the SS should be noted for the case $\theta = \theta_0 = 83^0$ and that is the fact that it reaches a minimum at 65 km and actually increases as we progress further from the top of the atmosphere and then falls abruptly to zero below 48 km. This behavior is understandable when we consider

the fact that the distance of closest approach (DCA) along the line of sight of the detector is 51.8 km, therefore there can't be any SS contributions below this level. Also for all levels above this altitude, SS constributions are coming from both sides of the DCA. Now as we move from the DCA toward the sub-solar point the transmission from the source to the scattering volume is increasing but the transmission from the scattering volume to the detector is decreasing at a faster rate. Another interesting feature is seen in the MS for this case. It is fairly uniform down to about 60 km and then rises in unison with the SS contribution and then falls precipitously below 50 km. This is in sharp contrast to the behavior of the MS contribution at the two smaller angles. For these cases the MS contribution is weakly monotonic decreasing from the top of the atmosphere. In Fig. 7b corresponding cases are presented except now $\tau = 1.0$. Now the optical thickness is large enough that the behavior exhibited by the SS at $\theta = \theta_o = 83^o$ for $\tau = 0.25$ is no longer present. Now it should be clear that the SS contribution for $\tau = 0.25$ can indeed be greater than the SS contribution for $\tau = 1.0$; a result which was alluded to earlier in the sequel. We should again emphasize the fact that this phenomenon can only occur in the SSA calculation and is totally prohibited by the PP approximation. The ratios of SS/TS for $\theta = \theta_o = 0, 60^o, 83^o$ are 21, 40 and 78% respectively, thus there is much more multiple scattering for $\tau = 0.25$ than for $\tau = 1.0$ at the smaller angles while at $\theta = \theta_o = 83^o$ the difference is much smaller, 83% compared to 78%. Thus it is clear that significantly different regions of the atmosphere are being probed as we view a planet over a wide range of phase angles.

In Table 3 we explore the violations of reciprocity for the SSA calculation, we first note that the SS results for the PP approximation satisfy reciprocity everywhere. Also the TS results satisfy reciprocity to within a few percent. These results are presented to give one an idea of the statistical fluctuations

to be expected in the SSA calculation since the same number of histories were run for corresponding angles. We also note that $I_{SS}^{SSA}(\mu, \mu_0, \phi)/I_{SS}^{SSA}(\mu_0, \mu, \phi)$ is independent of phase angle and deviations from the ratio of μ_0/μ are strictly due to curvature effects (see Table 2 of part 1 for Rayleigh scattering results). It is also apparent that the addition of MS makes matters worse. Also increasing the asymmetry of the phase function increases the discrepancy. This is physically what one would expect since the greater the asymmetry the further removed a photon will be from its point of injection before emergence.

Conclusions

We have examined the effects of sphericity on homogeneous conservative scattering atmospheres of optical depths τ = 0.25 and 1.0 with scattering according to a Henyey-Greenstein phase function for two values of the asymmetry factor, namely 0.5 and 0.7. Significant disagreement was found between the PP approximation and the more realistic SSA calculation. We also found that the degree of asymmetry strongly affects the radiance versus height distribution for multiple scattering. We have also shown that significantly different regions of the atmosphere are probed as one views a planet over a wide range of phase angles. These results will be useful for researchers in the fields of remote sensing and planetary spectroscopy. Violations of reciprocity also becomes more severe the more asymmetric the phase function.

Acknowledgement

This work was supported by Grant No. NGR-44-001-117 from the National Aeronautics and Space Administration. Acknowledgement is also made to the National Center for Atmospheric Research, which is sponsored by the National Science Foundation, for computer time used in this research.

Figure Captions

Figure 1 Comparison of Monte Carlo sampling of the Henyey-Greenstein phase function with the exact calculation.

Figure 2 Radiance versus nadir angle for a solar incident angle $\theta_0 = 0^0$. Open triangle is for spherical shell atmosphere calculation (SSA), solid circle is for the plane parallel calculation (PP) and MO is for the matrix operator plane parallel solutions. The dashed curve for the SSA case is simply drawn in to help guide the eye of the reader by smoothing out statistical fluctuations. All radiance values are normalized to a source strength of π per unit area perpendicular to the direction of propagation.

a) $\tau = 0.25$, $g = 0.5$; b) $\tau = 1.0$, $g = 0.5$; c) $\tau = 0.25$, $g = 0.7$; d) $\tau = 1.0$, $g = 0.7$

Figure 3 See caption to Fig. 2 except $\theta_0 = 70.47^0$ and the scan is done throughout the principal plane, $\phi = 0$ and 180^0.

Figure 4 Same as Figure 3 except $\theta_0 = 84.26^0$ and $g = 0.5$.

Figure 5 Same as Figure 4 except $g = 0.7$.

Figure 6 Radiance versus height distribution for both SS and MS for the SSA calculation for $\theta_0 = 0^0$, $\theta = 60^0$, and $\theta_0 = 60^0$, $\theta = 0^0$, and $\phi = 0^0$.

a) $\tau = 0.25$, $g = 0.5$; b) $\tau = 1.0$, $g = 0.5$; c) $\tau = 0.25$, $g = 0.7$; d) $\tau = 1.0$, $g = 0.7$

Figure 7 Radiance versus height distribution for both SS and MS for the following three cases: $\theta = \theta_0 = 0^0$, $\theta = \theta_0 = 60^0$, $\theta = \theta_0 = 83^0$, and $\phi = 0^0$.
a) $\tau = 0.25$, $g = 0.5$, b) $\tau = 1.0$, $g = 0.5$.

References

Adams, C. N. and Kattawar, G. W. (1977). "Radiative Transfer in Spherical Shell Atmospheres I. Rayleigh Scattering." Icarus (in press).

Table 1. Comparison of single scattering radiances from the backward, plane-parallel Monte Carlo calculations (I_{SS}^{PP}) with the backward, spherical shell Monte Carlo (I_{SS}^{SSA}). Also radiance ratios of single scattering to total scattering for the PP and SSA cases for various values of θ_0, θ, and ϕ, for $\tau = 0.25$ and 1.0 and $g = 0.5$ and 0.7. The minus sign and following integer gives the exponent of the power of ten multiplying the preceeding number.

$g = 0.5$

$\theta_0 = 0^0$

	$\tau = 0.25$				$\tau = 1.0$			
θ	I_{SS}^{PP}	I_{SS}^{SSA}	$I_{SS}^{SSA}/I_{TS}^{SSA}$ (%)	I_{SS}^{PP}/I_{TS}^{PP} (%)	I_{SS}^{PP}	I_{SS}^{SSA}	$I_{SS}^{SSA}/I_{TS}^{SSA}$ (%)	I_{SS}^{PP}/I_{TS}^{PP} (%)
0	1.09-2	1.09-2	56	55	2.40-2	2.40-2	21	20
10	1.12-2	1.12-2	56	55	2.45-2	2.45-2	22	21
20	1.20-2	1.20-2	55	55	2.60-2	2.61-2	22	21
30	1.36-2	1.36-2	55	55	2.89-2	2.89-2	21	22
40	1.62-2	1.63-2	55	55	3.34-2	3.35-2	22	22
50	2.07-2	2.09-2	56	56	4.04-2	4.06-2	23	23
60	2.85-2	2.90-2	54	54	5.13-2	5.17-2	25	24
70	4.35-2	4.53-2	55	56	6.82-2	6.89-2	27	27
80	7.67-2	9.84-2	58	59	9.39-2	9.51-2	35	34
85	1.07-1	1.10-1	67	62	1.12-1	1.13-1	42	40
88	1.24-1	8.66-2	74	67	1.24-1	1.25-1	49	48

$\theta_0 = 70.47^0$, $\phi = 0^0$

	$\tau = 0.25$				$\tau = 1.0$			
0	1.49-2	1.50-2	57	54	2.31-2	2.35-2	27	26
10	1.78-2	1.81-2	61	60	2.77-2	2.82-2	29	25
20	2.26-2	2.30-2	60	58	3.49-2	3.57-2	31	31
30	3.05-2	3.10-2	59	60	4.65-2	4.77-2	33	34
40	4.39-2	4.48-2	65	62	6.58-2	6.75-2	39	37
50	6.80-2	6.99-2	64	64	9.91-2	1.02-1	41	41
60	1.15-1	1.19-1	70	67	1.60-1	1.66-1	49	46
70	2.26-1	2.31-1	71	72	2.79-1	2.90-1	56	55
80	4.68-1	6.17-1	76	78	5.27-1	5.50-1	66	67
85	7.29-1	8.11-1	83	80	7.49-1	7.83-1	75	73
88	9.38-1	6.89-1	88	85	9.38-1	9.69-1	80	80

Table 1 Continued

$g = 0.5$

$\theta_o = 84.26^o$, $\phi = 0^o$

	$\tau = 0.25$				$\tau = 1.0$			
θ	I_{SS}^{PP}	I_{SS}^{SSA}	$I_{SS}^{SSA}/I_{TS}^{SSA}$ (%)	I_{SS}^{PP}/I_{TS}^{PP} (%)	I_{SS}^{PP}	I_{SS}^{SSA}	$I_{SS}^{SSA}/I_{TS}^{SSA}$ (%)	I_{SS}^{PP}/I_{TS}^{PP} (%)
0	1.01-2	1.22-2	59	56	1.09-2	1.22-2	37	38
10	1.27-2	1.53-2	58	65	1.35-2	1.53-2	36	39
20	1.68-2	2.03-2	61	65	1.79-2	2.03-2	38	45
30	2.37-2	2.88-2	62	68	2.52-2	2.86-2	43	51
40	3.58-2	4.39-2	69	70	3.80-2	4.32-2	49	54
50	5.81-2	7.20-2	69	73	6.15-2	7.02-2	54	57
60	1.02-1	1.29-1	73	76	1.08-1	1.23-1	60	64
70	1.97-1	2.57-1	77	79	2.06-1	2.36-1	67	72
80	4.36-1	7.07-1	81	84	4.44-1	5.12-1	76	79
85	7.21-1	1.025	86	86	7.24-1	8.35-1	82	83
88	1.05	9.16-1	90	89	1.05	1.20	87	88

$\theta_o = 70.47^o$, $\phi = 180^o$

	$\tau = 0.25$				$\tau = 1.0$			
0	1.49-2	1.50-2	57	57	2.31-2	2.35-2	27	26
10	1.31-2	1.32-2	56	54	2.03-2	2.06-2	25	25
20	1.21-2	1.22-2	52	51	1.87-2	1.89-2	24	24
30	1.18-2	1.19-2	52	52	1.80-2	1.82-2	22	23
40	1.22-2	1.23-2	51	51	1.83-2	1.85-2	21	23
50	1.35-2	1.36-2	50	52	1.96-2	1.97-2	20	23
60	1.60-2	1.63-2	49	45	2.24-2	2.24-2	20	19
70	2.12-2	2.18-2	44	45	2.74-2	2.74-2	23	22
80	3.28-2	3.79-2	42	45	3.13-2	3.71-2	27	24
85	4.38-2	4.69-2	52	48	4.05-2	4.59-2	33	29
88	5.19-2	3.80-2	59	52	5.19-2	5.32-2	43	38

Table 1 Continued

$g = 0.5$

$\theta_o = 84.26^o$, $\phi = 180^o$

	$\tau = 0.25$				$\tau = 1.0$			
θ	I_{SS}^{PP}	I_{SS}^{SSA}	$I_{SS}^{SSA}/I_{TS}^{SSA}$ (%)	I_{SS}^{PP}/I_{TS}^{PP} (%)	I_{SS}^{PP}	I_{SS}^{SSA}	$I_{SS}^{SSA}/I_{TS}^{SSA}$ (%)	I_{SS}^{PP}/I_{TS}^{PP} (%)
0	1.02-2	1.22-2	59	64	1.09-2	1.22-2	37	37
10	8.63-3	1.02-2	55	58	9.21-3	1.03-2	35	35
20	7.73-3	9.13-3	57	54	8.25-3	9.16-3	31	36
30	7.33-3	8.60-3	51	57	7.81-3	8.62-3	31	34
40	7.39-3	8.59-3	51	55	7.85-3	8.59-3	32	32
50	7.97-3	9.16-3	54	55	8.44-3	9.13-3	30	31
60	9.34-3	1.06-2	44	48	9.83-3	1.05-2	30	26
70	1.23-2	1.36-2	48	47	1.28-2	1.34-2	29	30
80	1.99-2	2.10-2	46	47	2.03-2	2.06-2	35	36
85	2.95-2	2.96-2	57	52	2.97-2	2.97-2	43	41
88	4.12-2	3.43-2	63	58	4.12-2	4.34-2	56	55

Table 2 same as Table 1 except g = 0.7

$g = 0.7$

$\theta_0 = 0^0$

	$\tau = 0.25$				$\tau = 1.0$			
θ	I_{SS}^{PP}	I_{SS}^{SSA}	$I_{SS}^{SSA}/I_{TS}^{SSA}$ (%)	I_{SS}^{PP}/I_{TS}^{PP} (%)	I_{SS}^{PP}	I_{SS}^{SSA}	$I_{SS}^{SSA}/I_{TS}^{SSA}$ (%)	I_{SS}^{PP}/I_{TS}^{PP} (%)
0	5.11-3	5.11-3	60	60	1.12-2	1.12-2	20	21
10	5.23-3	5.23-3	60	59	1.15-2	1.15-2	22	22
20	5.64-3	5.64-3	58	58	1.22-2	1.22-2	21	22
30	6.41-3	6.42-3	58	55	1.36-2	1.36-2	21	21
40	7.71-3	7.74-3	57	59	1.58-2	1.59-2	21	20
50	9.92-3	1.00-2	55	55	1.94-2	1.94-2	21	20
60	1.38-2	1.41-2	53	51	2.49-2	2.51-2	20	20
70	2.15-2	2.24-2	50	50	3.37-2	3.41-2	21	21
80	3.88-2	4.98-2	50	51	4.76-2	4.81-2	26	26
85	5.48-2	5.65-2	61	55	5.73-2	5.81-2	35	33
88	6.45-2	4.49-2	68	60	6.45-2	6.47-2	42	40

$\theta_0 = 70.47^0$, $\phi = 0^0$

	$\tau = 0.25$				$\tau = 1.0$			
0	7.36-3	7.44-3	47	48	1.14-2	1.16-2	22	22
10	9.05-3	9.16-3	50	50	1.40-2	1.43-2	21	22
20	1.19-2	1.20-2	51	51	1.83-2	1.87-2	20	23
30	1.67-2	1.70-2	56	48	2.54-2	2.61-2	26	24
40	2.55-2	2.60-2	50	54	3.82-2	3.92-2	25	27
50	4.30-2	4.42-2	54	51	6.26-2	6.45-2	27	29
60	8.22-2	8.54-2	55	53	1.14-1	1.18-1	30	32
70	1.85-1	1.98-1	56	58	2.39-1	2.49-1	37	38
80	5.25-1	6.93-1	62	63	5.92-1	6.18-1	52	52
85	9.78-1	1.09	76	70	1.00	1.05	63	62
88	1.42	1.04	86	77	1.42	1.47	76	73

Table 2 Continued

$g = 0.7$

$\theta_0 = 84.26^0$, $\phi = 0^0$

	$\tau = 0.25$				$\tau = 1.0$			
θ	I_{SS}^{PP}	I_{SS}^{SSA}	$I_{SS}^{SSA}/I_{TS}^{SSA}$ (%)	I_{SS}^{PP}/I_{TS}^{PP} (%)	I_{SS}^{PP}	I_{SS}^{SSA}	$I_{SS}^{SSA}/I_{TS}^{SSA}$ (%)	I_{SS}^{PP}/I_{TS}^{PP} (%)
0	5.21-3	6.23-3	56	50	5.57-3	6.24-3	26	30
10	6.74-3	8.11-3	46	52	7.20-3	8.11-3	27	36
20	9.38-3	1.13-2	50	57	1.00-2	1.13-2	30	35
30	1.42-3	1.72-2	53	50	1.51-2	1.71-2	29	39
40	2.36-3	2.89-2	50	59	2.50-2	2.85-2	34	46
50	4.41-2	5.47-2	58	58	4.67-2	5.33-2	40	49
60	9.60-2	1.21-1	60	63	1.01-1	1.16-1	44	53
70	2.53-1	3.29-1	64	70	2.63-1	3.02-1	52	60
80	8.49-1	1.38	73	76	8.66-1	9.98-1	66	71
85	1.75	2.49	83	81	1.76	2.03	77	79
88	2.87	2.49	90	86	2.87	3.25	86	85

$\theta_0 = 70.47^0$, $\phi = 180^0$

	$\tau = 0.25$				$\tau = 1.0$			
0	7.36-3	7.44-3	47	48	1.14-2	1.16-2	22	21
10	6.35-3	6.41-3	57	50	9.86-2	1.00-2	20	19
20	5.80-3	5.85-3	56	45	8.95-3	9.06-3	23	18
30	5.61-3	5.66-3	53	48	8.56-3	8.65-3	18	18
40	5.76-3	5.81-3	44	45	8.63-3	8.70-3	19	16
50	6.32-3	6.38-3	48	48	9.20-3	9.25-3	17	19
60	7.50-3	7.61-3	46	46	1.04-2	1.05-2	14	15
70	9.90-3	1.02-2	46	40	1.28-2	1.28-2	14	16
80	1.20-2	1.77-2	36	41	1.72-2	1.73-2	19	20
85	1.53-2	2.19-2	48	41	2.11-2	2.15-2	25	23
88	2.43-2	1.78-2	56	46	2.43-2	2.49-2	27	28

Table 2 Continued

$g = 0.7$

$\theta_o = 84.26^o$, $\phi = 180^o$

	$\tau = 0.25$				$\tau = 1.0$			
θ	I_{SS}^{PP}	I_{SS}^{SSA}	$I_{SS}^{SSA}/I_{TS}^{SSA}$ (%)	I_{SS}^{PP}/I_{TS}^{PP} (%)	I_{SS}^{PP}	I_{SS}^{SSA}	$I_{SS}^{SSA}/I_{TS}^{SSA}$ (%)	I_{SS}^{PP}/I_{TS}^{PP} (%)
0	5.21-3	6.23-3	53	50	5.57-3	6.24-3	26	30
10	4.30-3	5.11-3	43	56	4.60-3	5.13-3	30	28
20	3.78-3	4.47-3	47	42	4.04-3	4.48-3	25	25
30	3.53-3	4.14-3	46	50	3.76-3	4.15-3	22	26
40	3.52-3	4.09-3	43	41	3.74-3	4.09-3	24	26
50	3.76-3	4.33-3	44	51	3.99-3	4.31-3	20	21
60	4.39-3	4.97-3	42	46	4.62-3	4.92-3	17	21
70	5.77-3	6.37-3	37	38	6.01-3	6.27-3	21	20
80	9.32-3	9.80-3	39	43	9.50-3	9.60-3	26	30
85	1.38-2	1.38-2	49	48	1.39-2	1.39-2	38	31
88	1.93-2	1.60-2	54	51	1.93-2	2.03-2	43	38

Table 3. Reciprocity test for SS and TS for the PP and SSA cases for g = 0.5 and 0.7.

g = 0.5

τ = 0.25

μ_o	μ	ϕ	$\frac{I_{SS}^{PP}(\mu,\mu_o,\phi)}{I_{SS}^{PP}(\mu_o,\mu,\phi)}$	$\frac{I_{TS}^{PP}(\mu,\mu_o,\phi)}{I_{TS}^{PP}(\mu_o,\mu,\phi)}$	$\frac{I_{SS}^{SSA}(\mu,\mu_o,\phi)}{I_{SS}^{SSA}(\mu_o,\mu,\phi)}$	$\frac{I_{TS}^{SSA}(\mu,\mu_o,\phi)}{I_{TS}^{SSA}(\mu_o,\mu,\phi)}$	$\frac{\mu_o}{\mu}$
1.0	0.50	0	2.0	2.06	2.03	2.07	2.00
1.0	0.2588	0	3.86	3.94	4.07	4.04	3.85
1.0	0.12187	0	8.20	8.47	8.31	7.71	8.20
1.0	0.03490	0	28.6	30.6	9.90	7.74	28.6
0.50	0.2588	0	1.93	1.89	1.99	1.96	1.93
0.50	0.12187	0	4.10	4.11	4.08	3.97	4.10
0.50	0.0349	0	14.3	14.3	4.80	4.17	14.3
0.2588	0.12187	0	2.12	2.14	2.09	2.55	2.12
0.2588	0.0349	0	7.42	7.43	2.47	2.18	7.41
0.12187	0.0349	0	3.49	3.52	1.14	1.05	3.49
0.50	0.2588	180	1.93	1.89	2.01	2.06	1.93
0.50	0.12187	180	4.10	4.15	4.32	4.08	4.10
0.50	0.0349	180	14.3	14.3	5.72	4.83	14.3
0.2588	0.12187	180	2.12	2.17	2.21	2.20	2.12
0.2588	0.0349	180	7.41	7.11	3.53	2.83	7.41
0.12187	0.0349	180	3.49	3.28	2.21	2.07	3.49
				τ = 1.0			
1.0	0.50	0	2.00	1.99	2.00	2.01	2.00
1.0	0.2588	0	3.86	3.87	3.80	3.57	3.86
1.0	0.12187	0	8.21	8.17	7.59	6.89	8.20
1.0	0.0349	0	28.6	29.1	20.6	16.35	28.6
0.50	0.2588	0	1.93	1.86	1.89	1.84	1.93
0.50	0.12187	0	4.10	4.01	3.78	3.50	4.10
0.50	0.0349	0	14.3	13.8	10.2	8.74	14.3
0.2588	0.12187	0	2.12	2.18	2.00	1.92	2.12
0.2588	0.0349	0	7.41	7.45	5.39	4.85	7.41
0.12187	0.0349	0	3.49	3.46	2.69	2.54	3.49
0.50	0.2588	180	1.93	1.86	1.93	1.98	1.93
0.50	0.12187	180	4.10	4.08	3.97	3.51	4.10
0.50	0.0349	180	14.3	14.9	11.2	9.63	14.3
0.2588	0.12187	180	2.12	2.28	2.11	2.10	2.12
0.2588	0.0349	180	7.41	8.01	6.31	6.17	7.41
0.12187	0.0349	180	3.49	3.39	3.32	3.06	3.49

Table 3 Continued

$g = 0.7$

$\tau = 0.25$

μ_o	μ	ϕ	$\frac{I_{SS}^{PP}(\mu,\mu_o,\phi)}{I_{SS}^{PP}(\mu_o,\mu,\phi)}$	$\frac{I_{TS}^{PP}(\mu,\mu_o,\phi)}{I_{TS}^{PP}(\mu_o,\mu,\phi)}$	$\frac{I_{SS}^{SSA}(\mu,\mu_o,\phi)}{I_{SS}^{SSA}(\mu_o,\mu,\phi)}$	$\frac{I_{TS}^{SSA}(\mu,\mu_o,\phi)}{I_{TS}^{SSA}(\mu_o,\mu,\phi)}$	$\frac{\mu_o}{\mu}$
1.0	0.50	0	2.00	2.05	2.03	2.01	2.00
1.0	0.2588	0	3.86	3.96	4.07	4.37	3.86
1.0	0.12187	0	8.20	8.36	8.31	7.63	8.20
1.0	0.0349	0	28.6	30.4	9.90	7.05	28.6
0.50	0.2588	0	1.93	1.89	1.99	1.95	1.93
0.50	0.12187	0	4.10	4.00	4.08	3.63	4.10
0.50	0.0349	0	14.3	13.9	4.80	3.57	14.3
0.2588	0.12187	0	2.12	2.13	2.09	1.90	2.12
0.2588	0.0349	0	7.41	7.39	2.47	1.78	7.41
0.12187	0.0349	0	3.49	3.48	1.13	1.01	3.49
0.50	0.2588	180	1.93	1.82	2.01	2.07	1.93
0.50	0.12187	180	4.10	3.91	4.32	4.32	4.10
0.50	0.0349	180	14.3	14.1	5.72	3.32	14.3
0.2588	0.12187	180	2.12	2.07	2.21	2.48	2.12
0.2588	0.0349	180	7.41	7.28	3.53	2.13	7.41
0.12187	0.0349	180	3.49	3.31	2.21	1.59	3.49

$\tau = 1.0$

1.0	0.50	0	2.00	2.14	2.00	1.99	2.00
1.0	0.2588	0	3.86	4.04	3.80	3.59	3.86
1.0	0.12187	0	8.20	8.68	7.59	6.62	8.20
1.0	0.0349	0	28.6	28.6	20.6	14.5	28.6
0.5	0.2588	0	1.93	1.93	1.89	1.81	1.93
0.5	0.12187	0	4.10	4.19	3.78	3.24	4.10
0.5	0.0349	0	14.3	14.4	10.2	7.57	14.3
0.2588	0.12187	0	2.12	2.15	2.00	1.89	2.12
0.2588	0.0349	0	7.41	7.48	5.39	4.48	7.41
0.12187	0.0349	0	3.49	3.45	2.69	2.45	3.49
0.5	0.2588	180	1.93	1.83	1.93	1.78	1.93
0.5	0.12187	180	4.10	4.17	3.97	3.59	4.10
0.5	0.0349	180	14.3	13.7	11.2	8.80	14.3
0.2588	0.12187	180	2.12	2.27	2.11	1.81	2.12
0.2588	0.0349	180	7.41	7.81	6.31	5.21	7.41
0.12187	0.0349	180	3.49	3.47	3.32	3.24	3.49

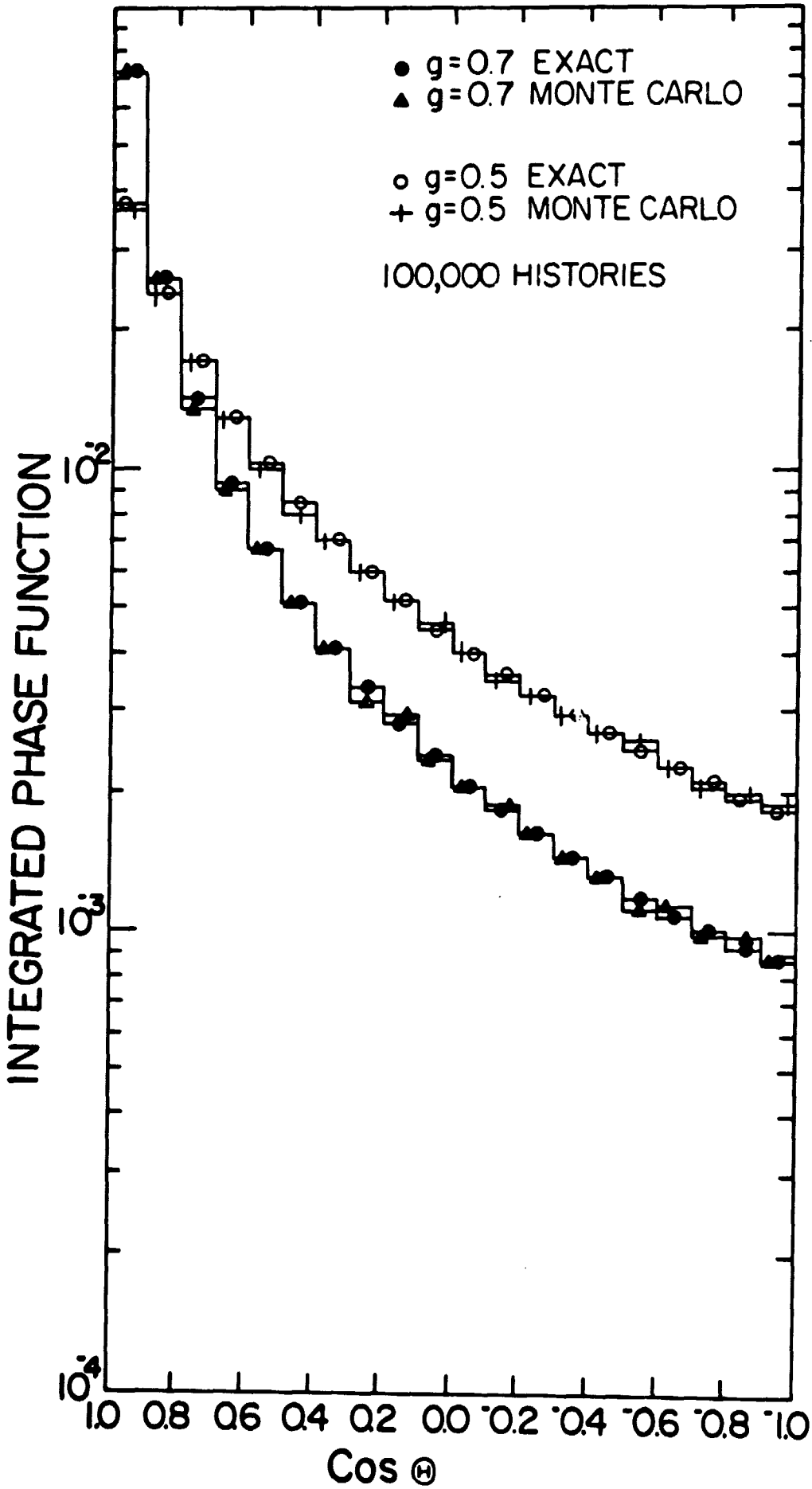
g=0.7 EXACT
g=0.7 MONTE CARLO
g=0.5 EXACT
g=0.5 MONTE CARLO
100,000 HISTORIES
INTEGRATED PHASE FUNCTION
10⁻²
10⁻³
10⁻⁴
1.0 0.8 0.6 0.4 0.2 0.0 -0.2 -0.4 -0.6 -0.8 -1.0
Cos Θ

Figure 1

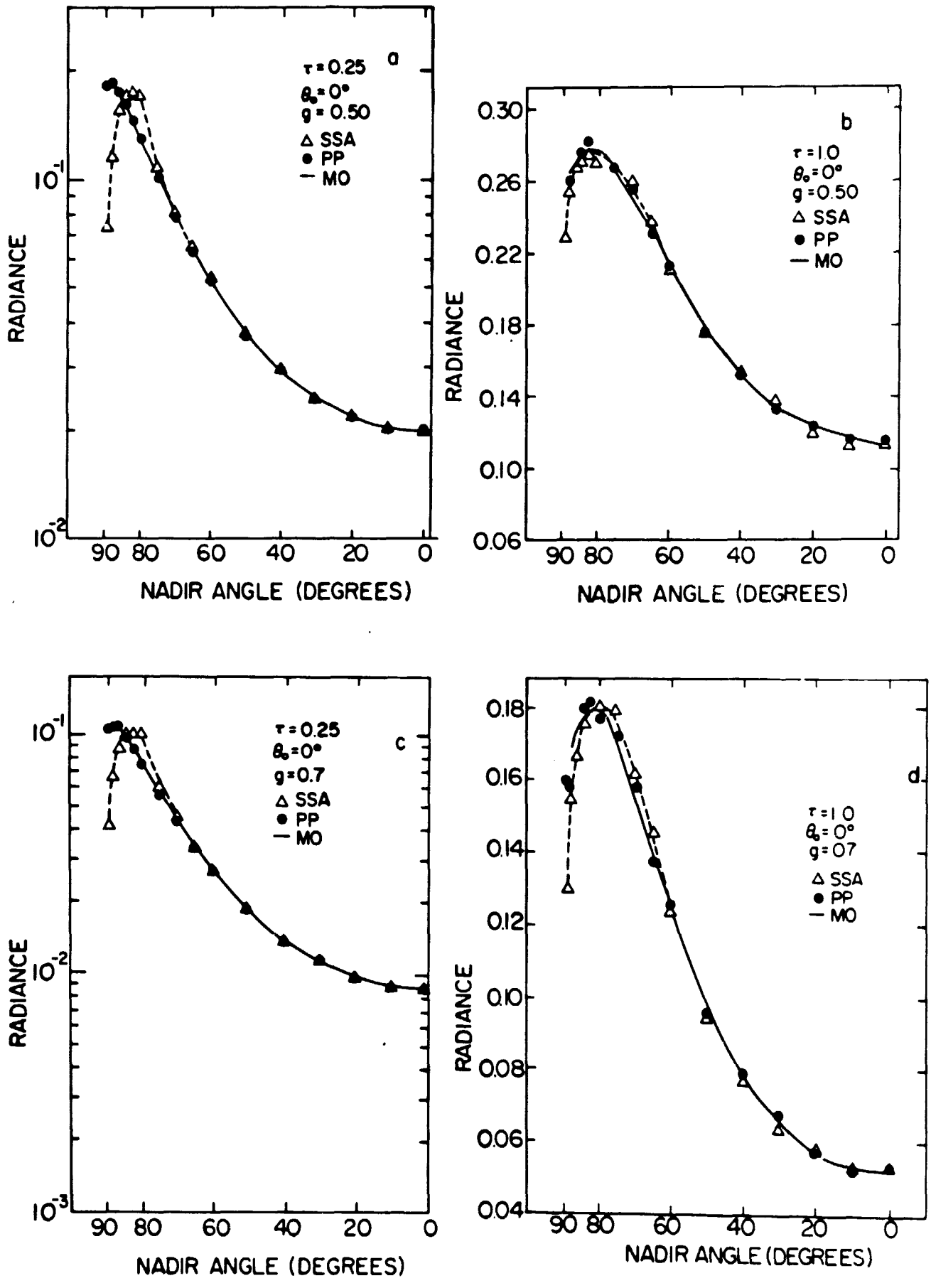
a
τ = 0.25
θ₀ = 0°
g = 0.50
Δ SSA
● PP
— MO
RADIANCE
NADIR ANGLE (DEGREES)
b
τ = 1.0
θ₀ = 0°
g = 0.50
Δ SSA
● PP
— MO
RADIANCE
NADIR ANGLE (DEGREES)
c
τ = 0.25
θ₀ = 0°
g = 0.7
Δ SSA
● PP
— MO
RADIANCE
NADIR ANGLE (DEGREES)
d
τ = 1.0
θ₀ = 0°
g = 07
Δ SSA
● PP
— MO
RADIANCE
NADIR ANGLE (DEGREES)

Figure 2

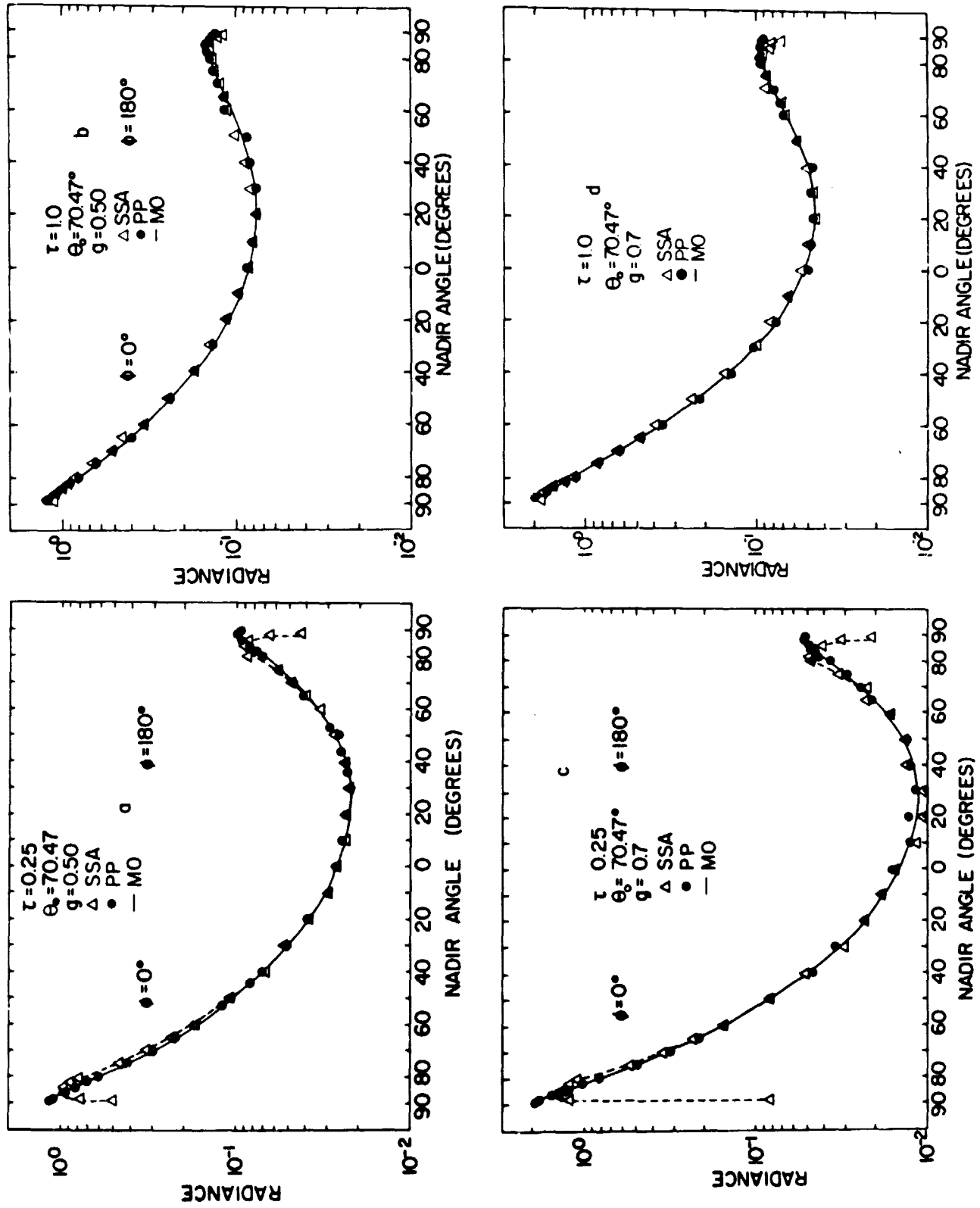
τ=0.25
θ₀=70.47
g=0.50
△ SSA
● PP
— MO
a
ϕ=0°
ϕ=180°
RADIANCE
NADIR ANGLE (DEGREES)
τ=1.0
θ₀=70.47°
g=0.50
△SSA
● PP
— MO
b
ϕ=0°
ϕ=180°
τ 0.25
θ₀= 70.47°
g= 0.7
△ SSA
● PP
— MO
c
τ=1.0
θ₀=70.47°
g=0.7
△ SSA
● PP
— MO
d

Figure 3

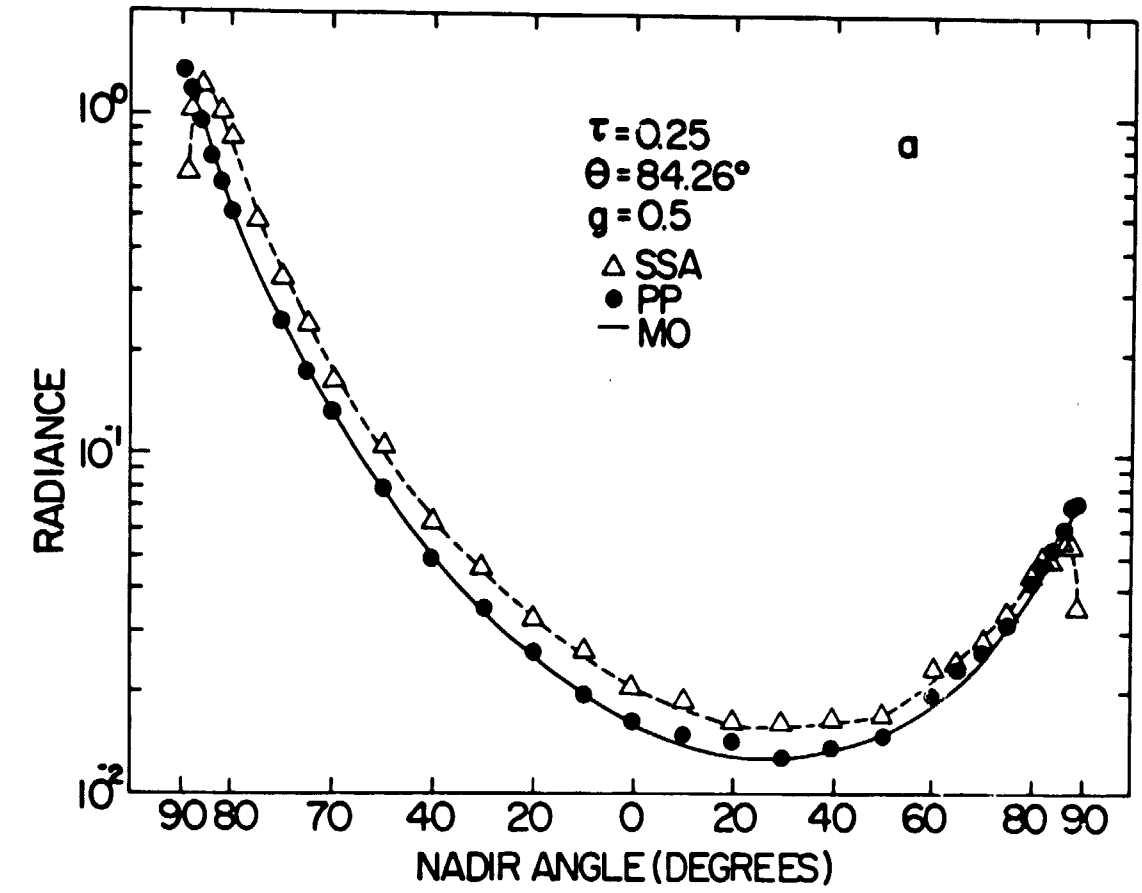
τ=0.25
θ=84.26°
g=0.5
△ SSA
● PP
— MO
a
RADIANCE
10^0
10^-1
10^-2
90 80 70 40 20 0 20 40 60 80 90
NADIR ANGLE (DEGREES)

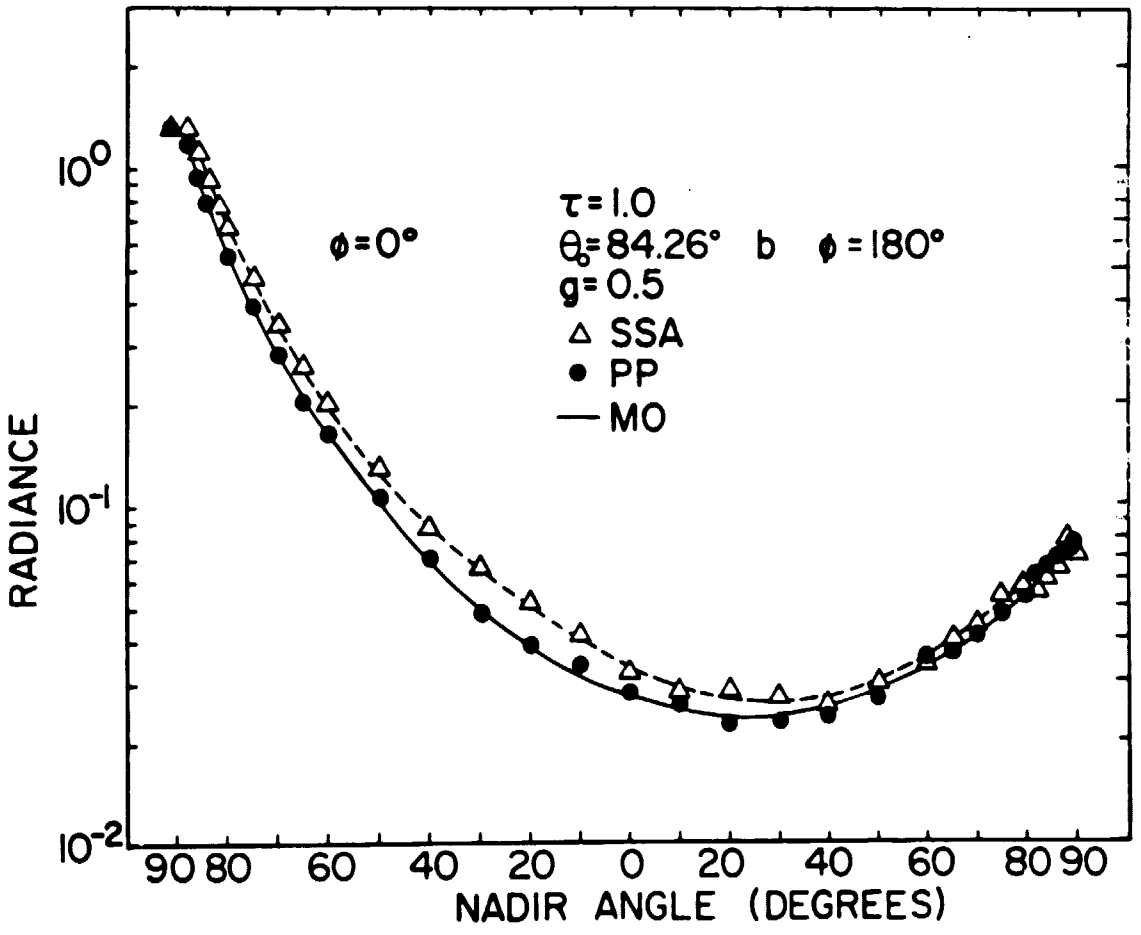
τ=1.0
θ₀=84.26°
g=0.5
△ SSA
● PP
— MO
φ=0°
b
φ=180°
RADIANCE
10^0
10^-1
10^-2
90 80 60 40 20 0 20 40 60 80 90
NADIR ANGLE (DEGREES)

Figure 4

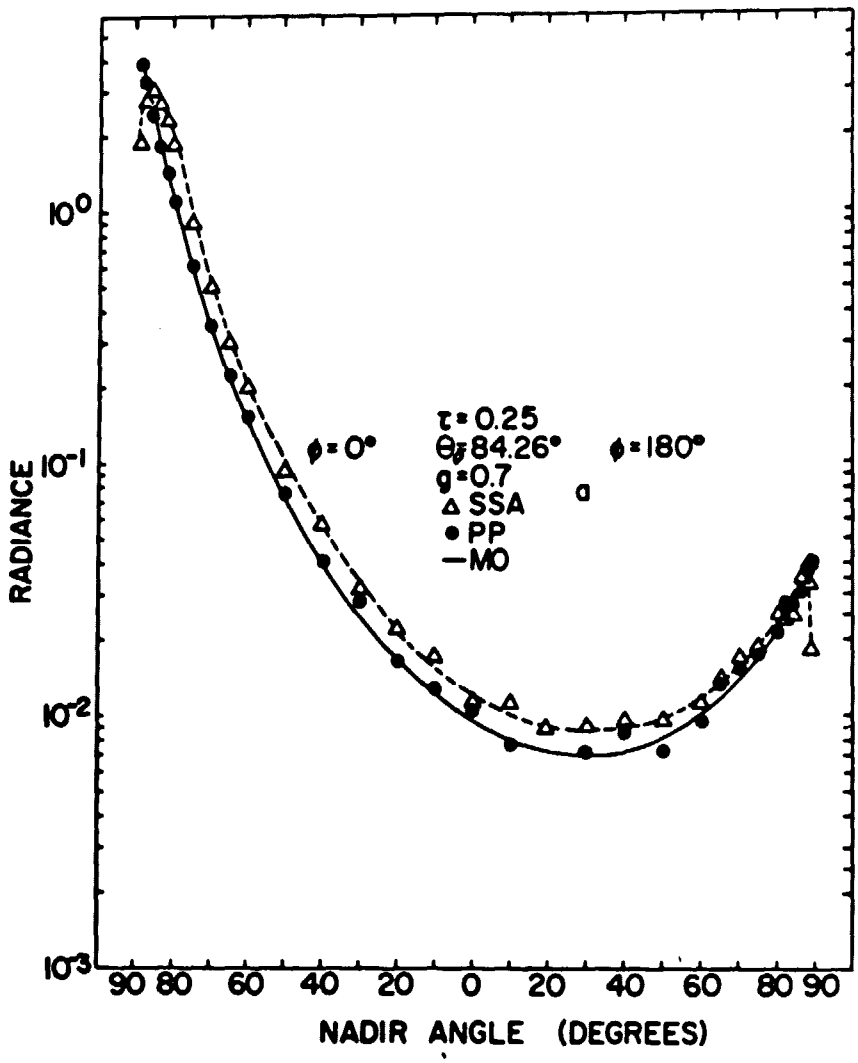
RADIANCE
10^0
10^{-1}
10^{-2}
10^{-3}
τ = 0.25
θ_0 = 84.26°
g = 0.7
Δ SSA
• PP
— MO
ϕ = 0°
ϕ = 180°
a
90 80 60 40 20 0 20 40 60 80 90
NADIR ANGLE (DEGREES)

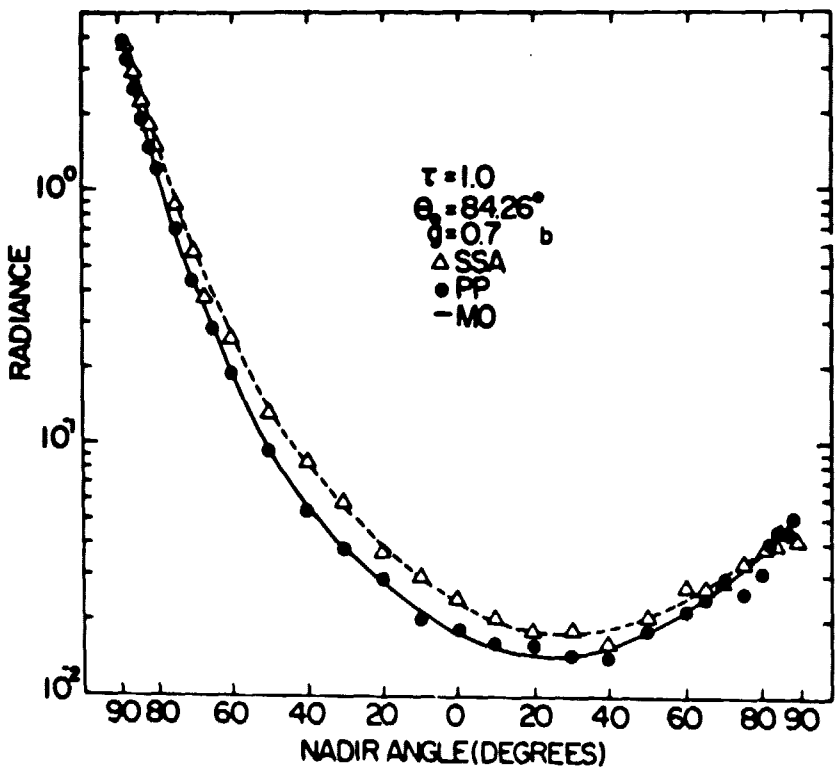
RADIANCE
10^0
10^1
10^2
τ = 1.0
θ_0 = 84.26°
g = 0.7
Δ SSA
• PP
— MO
b
90 80 60 40 20 0 20 40 60 80 90
NADIR ANGLE (DEGREES)

Figure 5

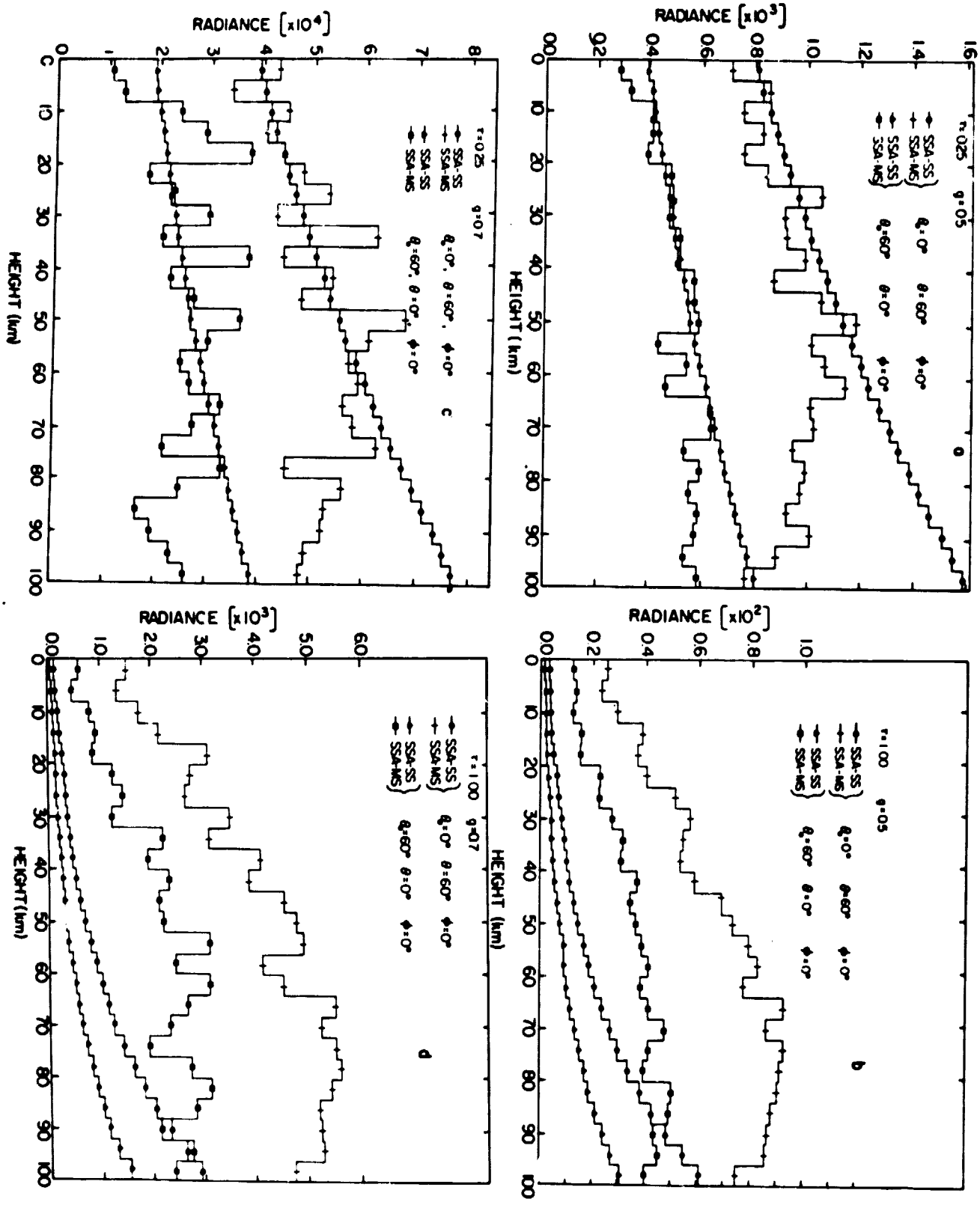
RADIANCE [x10³]
HEIGHT (km)
τ=.025 g=.05
SSA-SS
SSA-MS
θ=0° θ=60° φ=0°
θ=60° θ=0° φ=0°
a
RADIANCE [x10⁴]
HEIGHT (km)
τ=.025 g=.07
θ=0°, θ=60°, φ=0°
θ=60°, θ=0°, φ=0°
c
RADIANCE [x10²]
HEIGHT (km)
τ=1.00 g=.05
θ=0° θ=60° φ=0°
θ=60° θ=0° φ=0°
b
RADIANCE [x10³]
HEIGHT (km)
τ=1.00 g=.07
θ=0° θ=60° φ=0°
θ=60° θ=0° φ=0°
d

Figure 6

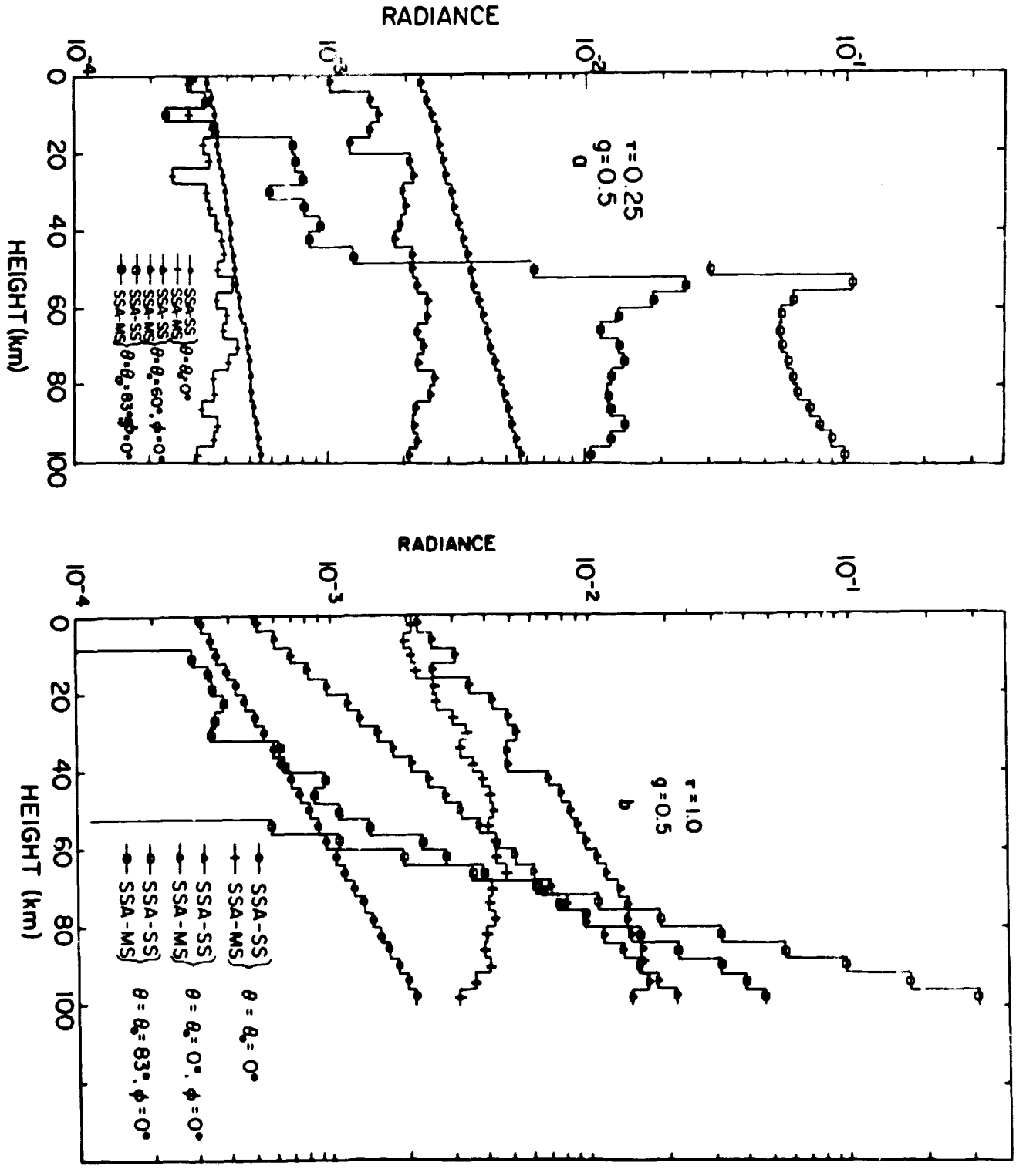
RADIANCE
10^{-4}
10^{-3}
10^{-2}
10^{-1}
HEIGHT (km)
0
20
40
60
80
100
τ=0.25
g=0.5
a
SSA-SS
SSA-MS
SSA-SS
SSA-MS
SSA-SS
SSA-MS
θ=θ₀=0°
θ=θ₀=60°, φ=0°
θ=θ₀=83°, φ=0°
RADIANCE
10^{-4}
10^{-3}
10^{-2}
10^{-1}
HEIGHT (km)
0
20
40
60
80
100
τ=1.0
g=0.5
b
SSA-SS
SSA-MS
SSA-SS
SSA-MS
SSA-SS
SSA-MS
θ = θ₀ = 0°
θ = θ₀ = 0°, φ = 0°
θ = θ₀ = 83°, φ = 0°

Figure 7